*6316–6322* *Nucleic Acids Research, 2009, Vol. 37, No. 19* *Published online 2 September 2009*
*doi:10.1093/nar/gkp702*

# Topological origins of chromosomal territories

**Julien Dorier and Andrzej Stasiak***

Center for Integrative Genomics, Faculty of Biology and Medicine, University of Lausanne, CH-1015, Switzerland

Received July 1, 2009; Revised August 5, 2009; Accepted August 9, 2009

## ABSTRACT

**Using freely jointed polymer model we compare equilibrium properties of crowded polymer chains whose segments are either permeable or not permeable for other segments to pass through. In particular, we addressed the question whether non-permeability of long chain molecules, in the absence of excluded volume effect, is sufficient to compartmentalize highly crowded polymer chains, similarly to what happens during formation of chromosomal territories in interphase nuclei. Our results indicate that even polymers without excluded volume compartmentalize and show strongly reduced intermingling when they are mutually non-permeable. Judging from the known fact that chromatin fibres originating from different chromosomes show very limited intermingling in interphase nuclei, we propose that regular chromatin fibres during chromosome decondensation can hardly serve as a substrate of cellular type II DNA topoisomerases.**

## INTRODUCTION

Upon finishing mitosis, chromosomes decondense into rather loose chromatin fibres and fill the entire cell nucleus. However, millimetre long chromatin fibres of individual chromosomes do not spread widely within several micrometer large cell nuclei but remain confined to semi-compact regions known as chromosome territories (1–4). What prevents long chromosome fibres of a given chromosome from spreading through the entire volume of the nucleus and from intermingling with chromatin fibres of other chromosomes? To appreciate this question one needs to realize that there are no membranes confining individual chromosome territories and that chromatin fibres are very dynamic (5). Until recently, complex biological mechanisms were proposed to be responsible for the creation of chromosome territories, such as binding to the nuclear matrix or participation of chromosome territory anchor proteins (1). However such hypothetical biological mechanisms may not be needed and the formation of chromosome territories could be simply entropy-driven, i.e. would occur spontaneously during equilibration of chromatin fibres under conditions where individual chromatin fibres do not pass through each other (6–8).

To explain why the restricted possibility of chromatin fibres to pass through each other should compress the chromosome fibres of individual chromosomes let us discuss briefly some earlier theoretical, numerical and experimental studies that were concerned with the effect of topological state of polymer chains on their equilibrium properties (9–11). These studies revealed that at high concentration, individual molecules of long circular polymers that are unlinked with each other tend to occupy rather compact regions with much smaller overall dimensions than the identical circular polymers in diluted solutions (9–11). Remarkably, that phenomenon is not observed in the case of highly concentrated linear polymers. Thus for example, long linear polymers under conditions where their segments neither attract nor repulse each other will on average keep the same spatial extent in highly concentrated and diluted solutions (9,11). What makes this difference between linear and circular polymers? In topological terms, linear polymers behave as if they were able to pass through each other. This results from the fact that every possible entanglement between two or more linear polymer molecules is possible even if the actual motion of the polymers required to achieve this state would necessitate passing around polymers' ends and that would take a very long time. On the other hand, circular polymers behave like mutually non-permeable chains and this excludes from the accessible configuration space all the configurations that would require formation of singly or multiply linked catenanes. As a consequence, mutually non-permeable circular polymers exclude each other (9–11). Therefore, for the entropic reasons, the most frequent configurations of highly concentrated circular polymers are expected to be compressed by the surrounding non-permeable circular polymers (9,10). The extent of this compression is somewhat controversial. Theoretical studies suggest a modest compression that in principle would permit some intermingling of neighbouring polymeric chains (9). Recent simulation studies postulated,

*To whom correspondence should be addressed. Tel: +41 21 692 4282; Fax: +41 21 692 4105; Email: andrzej.stasiak@unil.ch

however, that the expected compression should be strong and should lead to complete segregation of individual polymeric molecules (7,8,11).

Although earlier numerical simulation studies of highly concentrated circular polymers concluded that the mutual non-permeability of circular polymers causes that individual circular molecules get compacted, this conclusion was reached based on simulations of chains with very large effective diameter. For that reason the observed compression effect might result entirely or partially from the large excluded volume (geometrical exclusion) of the simulated circular chains.

To separate the effect of topological excluded volume (12–14) from the effect of geometrical excluded volume, we decided to compare equilibrium properties of crowded polygonal chains with the effective diameter of their segments set to zero, where segments were either free to pass through each other or not. It is important to add here that DNA under conditions of high charge neutralization, as it is the case in living cells, has very low effective diameter that can be nearly zero or even have negative values when the conditions are such that segments attract each other (15,16). Modelling of free passage conditions involves operating with phantom polygons which would correspond to a biological situation where type II DNA topoisomerases are highly active making sure that chromatin fibres could always freely pass through each other. Modelling conditions that do not allow intersegmental passages involves operating with non-phantom polygons, which approximate a hypothetical situation where type II DNA topoisomerases are practically unable to act on undistorted, healthy chromatin fibres. Such a biological setting would make good sense during chromosome decondensation as it would avoid unwanted DNA knotting that is known to interfere with such vital processes like DNA transcription and DNA replication (17,18). In addition, elimination of passages between chromatin fibres belonging to different chromosomes avoids topological problems during the process of chromatin condensation into mitotic chromosomes that need to be physically and topologically separated (6,19). Of course, there are processes where the action of type II DNA topoisomerases is necessary like the separation of freshly replicated daughter molecules (20,21) but it is known that chromatin structure of freshly replicated DNA are different from the regular interphase chromatin and this may signal DNA topoisomerases where to act (22,23). In fact, it was shown that type II DNA topoisomerases preferentially interact with regions that actually undergo DNA replication (24).

It needs to be stressed here that our simulations do not address a particular biological setting but investigate principal physical phenomena connected to dense packing of polymer molecules under conditions where they can freely pass or cannot pass through each other. We should expect that the magnitude of the effect connected to polymers non-permeability will in a given biological setting depend on the actual density of chromatin packing, chromosome size and other relevant characteristics of a given biological system, however the qualitative aspect should stay the same.

## MATERIALS AND METHODS

We studied systems composed of $M$ (from 2 to 20) freely jointed equilateral polygons each having $N$ (from 4 to 20) segments of length $l$ confined within a sphere of radius $2l$. Each segment is a hard-core cylinder with radius $10^{-5}l$ (i.e. the distance between two non-consecutive segments must be larger than $2 \times 10^{-5}l$). This very low effective diameter practically removed the excluded volume interactions between the segments and was computationally required to control the topology of the simulated polygons. The modelled system may seem to be much too small to reflect the chromatin packing in eukaryotic nuclei. However, with the setting where we model 20 freely jointed equilateral polygons, each composed of 20 segments and packed within the sphere having the diameter of four segments, we closely approach the situation within yeast nuclei. The estimations of the statistical segment length of chromatin fibres range between 130 and 270 nm, while the estimations of density of nucleosomes ranges from 3.6 to 6 per 11 nm (25). Therefore, assuming that the statistical segment length of chromatin is 250 nm, each statistical segment would contain ~115 nucleosomes, which will translate to about 23 000 bp. As a consequence each polygon composed of 20 statistical segments corresponds to 460 000 bp (that is a good size for an yeast chromosome as these range from 200 to 2200 kb), while all 20 modelled chains correspond to 9 200 000 bp packed within a sphere with a diameter of about 1 μm. Thus our simulation systems approach the situation in yeast nuclei that have the diameter of about 1.5 μm and contain 24 000 000 bp (per diploid genome). In fact the density of modelled chromatin in our system slightly exceeds this in yeast nuclei.

To sample the configuration space we used the Monte–Carlo algorithm described in (26,27). We only used crankshaft rotation moves, where randomly chosen subchains rotate along the line connecting first and last vertex of the subchain. In the case of phantom chains, the angle of rotation was randomly chosen between $-\pi$ and $\pi$ with uniform distribution. In the case of the non-phantom chains, we first determined the range of rotation angles such that the subchain did not cross any other segment during the rotation. The angle of rotation was then randomly chosen in this range with uniform distribution. For both phantom and non-phantom chains we did not accept new configurations resulting from crankshaft rotations that resulted in placing any vertex of the chain outside of the confinement sphere. For each simulation run with a given number of polygons $M$ and a given chain length $N$, we have evolved the system over $2 \times 10^9$ crankshaft rotations. The first $1 \times 10^6$ configurations were not entered into the statistics.

To generate initial configurations, we started with each polygon in a regular N-gon configuration, stacked on top of each other. We added an energy given by the sum of the squared distance from all the vertices to the centre of the sphere. The Monte–Carlo Metropolis algorithm with non-phantom chains described previously was then used with slowly decreasing temperature until all the polygons were

inside the sphere (see Figure S1A). Note that the initial configurations obtained with this procedure are unknotted and uncatenated.

We have checked that the reached equilibrium state was independent from the initial conditions by performing several simulation runs in which initial configurations were built out of highly compacted individual polygons well separated from each other (Figure S1B).

It is important to add here that Monte–Carlo simulations such as those used by us are unsuited to follow the evolution or kinetics of the investigated system. However, after sufficient equilibration time, the generated configurations sample in a very efficient and non-biased way the configuration space accessible to modelled physical system such as DNA molecules or chromatin fibres (26,28,29). In addition this type of simulations allow much better characterization of the equilibrium than simulation approaches that permit to follow the evolution of the system and thus give information concerning the kinetics.

## RESULTS

### Effect of topological restriction on the size of modelled polymeric chains

To investigate effects of mutual non-permeability of modelled polymer chains on their spatial extent, we proceeded with Monte–Carlo simulations to characterize equilibrium properties of permeable (phantom) and non-permeable (non-phantom) sets of freely jointed polygonal chains that were placed within a small sphere (having the radius of two segment lengths). Spherical confinement was applied to mimic the interior of cell nuclei that usually have quasi-spherical shape. To measure overall spatial dimensions of modelled polygons we have calculated their radius of gyration $R_g$, which is the root mean square distance of the vertices of a given polygon from the centre of mass of this polygon

Figure 1 shows typical snapshots of equilibrated configurations adopted by highly crowded sets composed of 20 polygonal chains with 20 segments each that are either phantom (left) or non-phantom (right). To improve the visibility of the modelled polygons the diameter of each segment is highly enlarged as compared to the actual diameter set during the simulations. A closer inspection of Figure 1 reveals that in the case of phantom chains (left) the centre of the sphere is highly crowded with many chains being topologically linked there while more of free space can be found towards the sphere's periphery. In the non-phantom case (right) the polygonal chains fill the space more uniformly as would be expected if they experience mutual topological exclusion. Notice that in the set of polygons shown in Figure 1B there are no interlinking between different chains and no knotting of individual chains.

To investigate the effect of chain length and of crowding on the $R_g$ of phantom and non-phantom chains we studied equilibrated systems where the length and the number of chains confined to the same size sphere varies. Figure 2 presents the results of these studies. We can clearly see the topological compression effect. In addition, as the number of chains increases the topological compression effect becomes stronger. Most likely the effect would still get stronger with a higher number of chains but the simulation time required to investigate more crowded states was prohibitively long.

### Effect of topological restriction on the intermingling of modelled polymeric chains

We wanted to measure the intermingling of modelled polygonal chains in a way resembling the methodology used to demark chromosome territories on optical

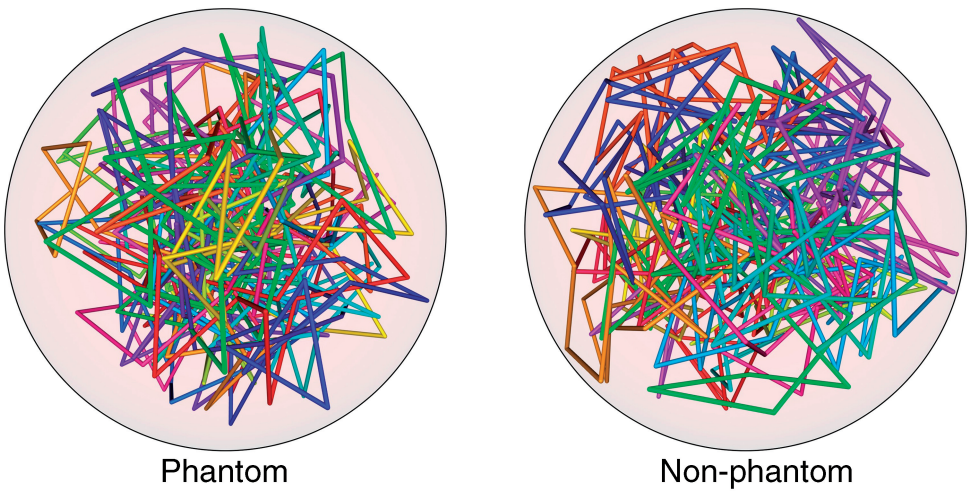


**Figure 1.** Snapshots of equilibrated configurations of strongly crowded 20 freely jointed polygons (each composed of 20 segments) that are either phantom (left) or non-phantom i.e. keeping the topology of uncatenated and unknotted circles (right). In both cases the polygons are confined within spheres having the radius of two segment lengths ($l$). Notice that the non-phantom polygons (right) are distributed more uniformly than the phantom polygons that show the tendency to share the space in the centre of the sphere. To facilitate visualization of position and form of individual polygons the diameter of the segments was greatly increased as compared to actually simulated polygons.

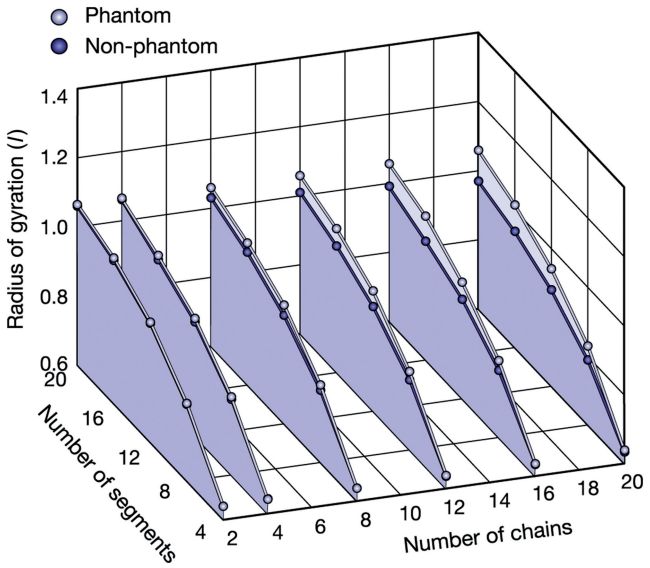


**Figure 2.** Radius of gyration (in units of segment length $l$) of non-phantom polygons decreases with their crowding. $R_g$ values for phantom and non-phantom polygons as the function of the number of polygons and the number of segments in each polygon. While phantom polygons do not change their overall spatial dimensions with the increasing chain numbers (as expected), the non-phantom polygons become progressively compressed by the presence of other non-phantom polygons. The error bars are smaller than data point symbols.

cross-sections through cell nuclei (1). The optical microscopy approach consist first of 'painting' chromatin fibres originating from individual chromosomes with different fluorescence dyes using chromosome-specific hybridization probes. The territories are demarked then on optical cross sections as regions showing strong predominance of one colour (30). The corresponding procedure applied to our modelled polygonal chains consists of giving different colours to different polygons and determining intersections of individual polygons with the equatorial plane of the sphere of confinement (Figure 3A). Subsequently, polygon-specific convex envelopes are determined that enclose all the intersection points of a given polygon within the equatorial plane (Figure 3B). Finally as the intermingling value we take the ratio between the total area of all intersections of polygon-specific 2D convex envelopes (dark-grey areas in Figure 3C) and the total area of all polygon-specific 2D convex envelopes (Figure 3C). The intermingling values can range from zero (no intermingling) to 1 (complete intermingling). Figure 4A compares the intermingling in phantom and non-phantom chains as a function of the number of chains and the number of segments in individual polygons. As it is shown on the figure, the intermingling in phantom chains is always bigger than in the corresponding case of non-phantom chains although the intermingling increases both in phantom and non-phantom chains with the increasing crowding (increasing number of segments in the sphere of confinement). It is important to note here that real chromosome territories also show significant overlaps indicating that a limited

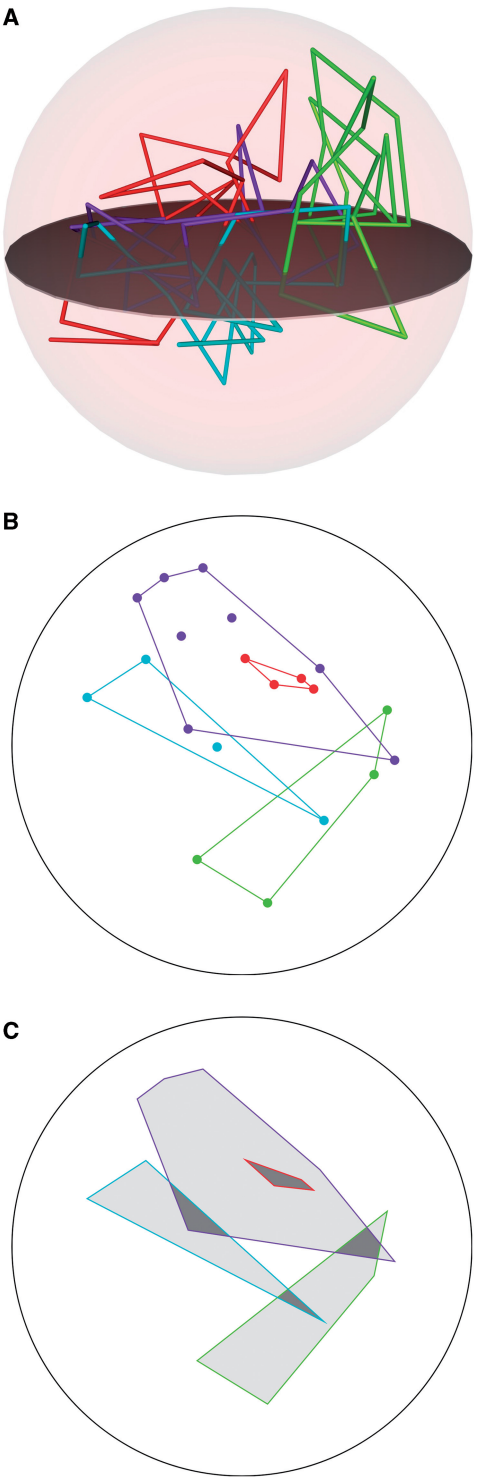


**Figure 3.** Polygon's intermingling: what is it and how to measure it? (**A**) To measure the intermingling between distinct polygonal chains we first determine the points of intersection of these chains with an equatorial plane. (**B**) Subsequently, we determine for each polygonal chain the 2D convex envelope enclosing all intersections points of a given polygonal chain with the equatorial plane. (**C**) Finally, we calculate the ratio of the total area of all intersections of the convex envelopes (marked as dark grey) to the total surface area of all convex envelopes. This ratio may range from 0 to 1 and expresses the extent of the intermingling.

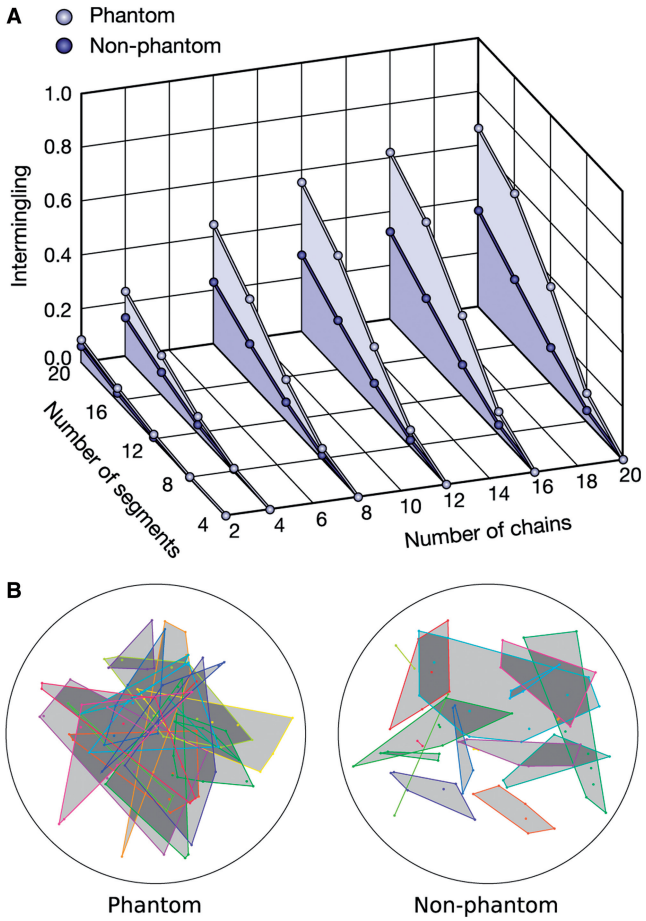


**Figure 4.** Non-phantom polygons show greatly reduced intermingling as compared with phantom polygons. (**A**) Intermingling values for phantom and non-phantom polygons as the function of the number of polygons and the number of segments in each polygon. The error bars are smaller than data point symbols. (**B**) Equatorial cross-sections corresponding to the snapshots presented in Figure 1. Notice strong intermingling in case of phantom polygons (left) and mostly spatially separated cross sections of the individual 'territories' in the case of non-phantom polygons (right).

intermingling is common (4). Figure 4B shows the equatorial cross-section corresponding to the snapshots shown in Figure 1. It is clearly visible that phantom chains show much higher intermingling than non-phantom chains.

## DISCUSSION

Our simulation studies investigated whether the mere inability of polymer chains to pass through each other could compress highly concentrated circular polymers even if they had negligible geometrical excluded volume. The regime of very thin non-phantom polymers is biologically significant since the effective diameter of DNA under conditions of efficient charge screening is close to zero or even can have negative values when DNA segments attract each other as in the presence of physiological concentrations of counterions that can interact with DNA *in vivo* (15,16). We have observed that the mere inability of circular polymers to pass through each other induces the topological compression effect that could explain why individual decondensed chromosomes do not spread through the entire available volume of cell nucleus but form chromosome territories. Several recent numerical studies postulated important role of topological restriction in inducing strong spatial confinement of long circular polymers (7,8,11). However, those earlier studies operated with a model that associates large excluded volume (of the order of segment length) to modelled polymeric chains. That raised a possibility that large excluded volume of ring polymers may be needed to induce mutual compactions in highly concentrated solutions. Our study shows that the topological restriction alone is sufficient to induce mutual compaction of ring polymers.

In our simulations we have used circular polygons since in a strict sense topological restrictions can only apply to closed topological domains. However, eukaryotic chromosomes are linear. Why then should the linear chromosomes behave like non-penetrable circular polymers? Several papers have reported that chromatin fibres are forming large loops closed by interaction with specific proteins (3,31), in addition specific regions of chromosomes such as centromeres and telomeres show attachments to the nuclear membrane (5,32). Formation of loops involving chromatin fibres of individual chromosomes or formation of points of stable contact with the nuclear membrane effectively convert linear chromatin fibres into closed topological loops that would exclude each other provided that type II DNA topoisomerases do not act on them.

Of course, the topological compression is only observed for non-phantom chains and this implies that free DNA–DNA passages would have to be strongly restricted during chromosome decondensation to be able to contribute to formation of chromosome territories. This restriction of DNA–DNA passages contrasts though with a frequent assumption that type II DNA topoisomerases, present in all healthy living cells, effectively make the chromatin fibres permeable to each other. However, this assumption is not supported by experimental data revealing that the activity of type DNA topoisomerases on unperturbed chromatin fibres *in vivo* is in fact strongly restricted (33,34). The question arises then what would activate type II DNA topoisomerases when their action is necessary, like it is the case during the separation of freshly replicated daughter DNA molecules that form precatenanes and catenanes (the later only occur in case of circular chromatin fibres like these formed by SV40 mini-chromosomes)? Since freshly replicated chromatin has a different structure than the structure of 'established' chromatin fibres (22,23) it would probably make a good sense if type II DNA topoisomerases were specifically recognizing freshly replicated chromatin fibres but neglecting the 'established' fibres.

Once we accept the possibility that normal chromatin fibres hardly serve as substrates for type II DNA topoisomerases, we may consider what would happen if chromosomes were decondensing to long linear chromatin fibres that were free from any loops or attachment points to nuclear membrane [although we know that this is not the case (3,5,31,32)]. At the equilibrium such fibres

should perfectly intermingle. But, what would be the time needed to reach such an equilibrium? As already mentioned, our simulation approach is not suited to evaluate the real kinetics of the system. However, molecular dynamics type of simulations performed by Rosa and Everaers (6) addressed this question and arrived to a conclusion that the equilibration time for long chromatin fibres forming human chromosomes would amount to staggering 500 years. With such a long time of equilibration even linear chromatin fibres that are sufficiently long should form clearly defined chromosomal territories during all biological observations that are mostly concerned with the time periods of several hours or days after the chromosome decondensation. However, this would only be the case if these chromatin fibres were 'immune' to type II DNA topoisomerases.

If the time needed for the equilibration can be so long how this would affect our conclusion that topological effects are responsible for formation of chromosomal territories? It would not change our conclusions since the long equilibration time of long linear chromatin fibres results from the topological effect, i.e. the assumed inability of the fibres to pass through each other. If one would assume free passages the equilibration time would be short.

If the kinetics of long chromatin fibres in the absence of intersegmental passages is so slow, how relevant are then our simulation results for the situation at the equilibrium? Interestingly, the opposition to intermingling would be even stronger before the equilibration is reached (6). Therefore, our results may only underestimate the real territorialization of chromosomes.

Another possible consequence of slow equilibration kinetics of long chromatin fibres is that some limited topo II activity permitting rare passages between chromatin fibres belonging to different chromosomes may still be compatible with chromosomal territories being observed several hours or days after chromosome decondensation.

Is there biological evidence for the proposal that topological effects are responsible for the formation of chromosomal territories? Double-stranded DNA breaks should be able to release the DNA from the topological constraint and the cut chromatin fibres should be able to invade surrounding territories using created free ends. Indeed, many papers reported local chromatin expansion around the double-stranded break site [for a recent discussion, see ref. (35)]. However, in all analysed cases it is difficult to say whether the observed movement is a simple consequence of the emergence of free ends or whether this movement is the result of specific chromatin remodelling involved in the signalling and repair of double-stranded DNA breaks. Perhaps the most suggestive result was reported by Kruhlak *et al.* who observed that specifically labelled chromatin regions surrounding double-stranded breaks expand by 30–40% within 180 s following the emergence of double-stranded breaks (36). This observation is consistent with the idea that double-stranded breaks release the cut DNA from the topological constraint and permit then the invasion of surrounding chromatin territories. However, more studies are needed to verify how important is the entropic effect connected to mutual non-permeability of chromatin fibres.

## CONCLUSIONS

Using a simple model system, we have provided a proof of principle that even under conditions where the effective diameter of DNA and of formed chromatin fibres is very small, the mere restriction of DNA–DNA passages can lead to formation of chromosome territories.

## ACKNOWLEDGEMENTS

The authors thank Vital-IT (www.vital-it.ch), the computational biology platform of Swiss Bioinformatics Institute for making available their computational resources for our calculations.

## FUNDING

Swiss NSF grant [3100A0-116275 to A.S.].

*Conflict of interest statement*. None declared.

## REFERENCES

1. Cremer,T. and Cremer,C. (2001) Chromosome territories, nuclear architecture and gene regulation in mammalian cells. *Nat. Rev. Genet.*, **2**, 292–301.
2. Tanabe,H., Muller,S., Neusser,M., von Hase,J., Calcagno,E., Cremer,M., Solovei,I., Cremer,C. and Cremer,T. (2002) Evolutionary conservation of chromosome territory arrangements in cell nuclei from higher primates. *Proc. Natl Acad. Sci. USA*, **99**, 4424–4429.
3. Cremer,T., Cremer,M., Dietzel,S., Muller,S., Solovei,I. and Fakan,S. (2006) Chromosome territories – a functional nuclear landscape. *Curr. Opin. Cell Biol.*, **18**, 307–316.
4. Branco,M.R. and Pombo,A. (2006) Intermingling of chromosome territories in interphase suggests role in translocations and transcription-dependent associations. *PLoS Biol.*, **4**, e138.
5. Gasser,S.M. (2002) Visualizing chromatin dynamics in interphase nuclei. *Science*, **296**, 1412–1416.
6. Rosa,A. and Everaers,R. (2008) Structure and dynamics of interphase chromosomes. *PLoS Comput. Biol.*, **4**, e1000153.
7. de Nooijer,S., Wellink,J., Mulder,B. and Bisseling,T. (2009) Non-specific interactions are sufficient to explain the position of heterochromatic chromocenters and nucleoli in interphase nuclei. *Nucleic Acids Res.*, **37**, 3558–3568.
8. Vettorel,T., Grosberg,A.Y. and Kremer,K. (2009) Statistics of polymer rings in the melt: a numerical study. *Phys. Biol.*, **6**, 25013.
9. Cates,M.E. and Deutsch,J.M. (1986) Conjectures on the statistics of ring polymers. *J. Physique*, **47**, 2121–2128.
10. Müller,M., Wittmer,J.P. and Cates,M.E. (1996) Topological effects in ring polymers: a computer simulation study. *Phys. Rev. E*, **53**, 5063–5074.
11. Suzuki,J., Takano,A. and Matsushita,Y. (2008) Topological effect in ring polymers investigated with Monte Carlo simulation. *J. Chem. Phys.*, **129**, 034903.
12. Deutsch,J.M. (1999) Equilibrium size of large ring molecules. *Phys. Rev. E*, **59**, R2539–R2541.
13. Dobay,A., Dubochet,J., Millett,K., Sottas,P.E. and Stasiak,A. (2003) Scaling behavior of random knots. *Proc. Natl Acad. Sci. USA*, **100**, 5611–5615.
14. Moore,N.T., Lua,R.C. and Grosberg,A.Y. (2004) Topologically driven swelling of a polymer loop. *Proc. Natl Acad. Sci. USA*, **101**, 13431–13435.
15. Shaw,S.Y. and Wang,J.C. (1993) Knotting of a DNA chain during ring closure. *Science*, **260**, 533–536.

16. Bednar,J., Furrer,P., Stasiak,A., Dubochet,J., Egelman,E.H. and Bates,A.D. (1994) The twist, writhe and overall shape of supercoiled DNA change during counterion-induced transition from a loosely to a tightly interwound superhelix. Possible implications for DNA structure in vivo. *J. Mol. Biol.*, **235**, 825–847.
17. Portugal,J. and Rodriguez-Campos,A. (1996) T7 RNA polymerase cannot transcribe through a highly knotted DNA template. *Nucleic Acids Res.*, **24**, 4890–4894.
18. Deibler,R.W., Mann,J.K., Sumners,D.W. and Zechiedrich,L. (2007) Hin-mediated DNA knotting and recombining promote replicon dysfunction and mutation. *BMC Mol. Biol.*, **8**, 44.
19. Sikorav,J.L. and Jannink,G. (1994) Kinetics of chromosome condensation in the presence of topoisomerases: a phantom chain model. *Biophys. J.*, **66**, 827–837.
20. Schvartzman,J.B. and Stasiak,A. (2004) A topological view of the replicon. *EMBO Rep.*, **5**, 256–261.
21. Nitiss,J.L. (2009) DNA topoisomerase II and its growing repertoire of biological functions. *Nat. Rev. Cancer*, **9**, 327–337.
22. Gasser,R., Koller,T. and Sogo,J.M. (1996) The stability of nucleosomes at the replication fork. *J. Mol. Biol.*, **258**, 224–239.
23. Krude,T. (1999) Chromatin assembly during DNA replication in somatic cells. *Eur. J. Biochem.*, **263**, 1–5.
24. Bermejo,R., Doksani,Y., Capra,T., Katou,Y.M., Tanaka,H., Shirahige,K. and Foiani,M. (2007) Top1- and Top2-mediated topological transitions at replication forks ensure fork progression and stability and prevent DNA damage checkpoint activation. *Genes Dev.*, **21**, 1921–1936.
25. Dekker,J. (2008) Mapping in vivo chromatin interactions in yeast suggests an extended chromatin fiber with regional variation in compaction. *J. Biol. Chem.*, **283**, 34532–34540.
26. Vologodskii,A.V., Levene,S.D., Klenin,K.V., Frank-Kamenetskii,M. and Cozzarelli,N.R. (1992) Conformational and thermodynamic properties of supercoiled DNA. *J. Mol. Biol.*, **227**, 1224–1243.
27. Burnier,Y., Dorier,J. and Stasiak,A. (2008) DNA supercoiling inhibits DNA knotting. *Nucleic Acids Res.*, **36**, 4956–4963.
28. Burnier,Y., Weber,C., Flammini,A. and Stasiak,A. (2007) Local selection rules that can determine specific pathways of DNA unknotting by type II DNA topoisomerases. *Nucleic Acids Res.*, **35**, 5223–5231.
29. Wedemann,G. and Langowski,J. (2002) Computer simulation of the 30-nanometer chromatin fiber. *Biophys. J.*, **82**, 2847–2859.
30. Bolzer,A., Kreth,G., Solovei,I., Koehler,D., Saracoglu,K., Fauth,C., Muller,S., Eils,R., Cremer,C., Speicher,M.R. *et al.* (2005) Three-dimensional maps of all chromosomes in human male fibroblast nuclei and prometaphase rosettes. *PLoS Biol.*, **3**, e157.
31. Munkel,C., Eils,R., Dietzel,S., Zink,D., Mehring,C., Wedemann,G., Cremer,T. and Langowski,J. (1999) Compartmentalization of interphase chromosomes observed in simulation and experiment. *J. Mol. Biol.*, **285**, 1053–1065.
32. Rosa,A., Maddocks,J.H., Neumann,F.R., Gasser,S.M. and Stasiak,A. (2006) Measuring limits of telomere movement on nuclear envelope. *Biophys. J.*, **90**, L24–L26.
33. Lavelle,C. (2008) DNA torsional stress propagates through chromatin fiber and participates in transcriptional regulation. *Nat. Struct. Mol. Biol.*, **15**, 123–125.
34. Kouzine,F., Sanford,S., Elisha-Feil,Z. and Levens,D. (2008) The functional response of upstream DNA to dynamic supercoiling in vivo. *Nat. Struct. Mol. Biol.*, **15**, 146–154.
35. Jakob,B., Splinter,J., Durante,M. and Taucher-Scholz,G. (2009) Live cell microscopy analysis of radiation-induced DNA double-strand break motion. *Proc. Natl Acad. Sci. USA*, **106**, 3172–3177.
36. Kruhlak,M.J., Celeste,A., Dellaire,G., Fernandez-Capetillo,O., Muller,W.G., McNally,J.G., Bazett-Jones,D.P. and Nussenzweig,A. (2006) Changes in chromatin structure and mobility in living cells at sites of DNA double-strand breaks. *J. Cell Biol.*, **172**, 823–834.